8th U. S. National Combustion Meeting
Organized by the Western States Section of the Combustion Institute
and hosted by the University of Utah
May 19-22, 2013

Pyrolysis and CO_2 Gasification Rates of Biomass at High Heating Rate Conditions

Aaron D. Lewis, Emmett G. Fletcher, and Thomas H. Fletcher[1]

[1]*Department of Chemical Engineering, Brigham Young University, Provo, Utah 84602, USA*

The pyrolysis and CO_2 gasification of four biomass feed stocks (Poplar sawdust, straw, switchgrass, and corn stover) were studied at conditions of high initial particle heating rates (~10^5 K/s) using two flat-flame burner reactors. The chosen feed stocks include energy crops as well as both woody and agricultural residues. Pyrolysis experiments were performed using four biomass samples (45-75 μm) in a flat-flame burner reactor at atmospheric pressure. The peak gas temperature and range of particle residence times in these pyrolysis experiments was 1163 K and 34-113 ms. The pyrolysis yields of tar, char, and light gas are reported as a function of time in the reactor. The mass release of the fully-pyrolyzed biomass samples from the flat-flame reactor exceeded their respective ASTM volatiles value by 7.0 to 11.6 wt% (dry, ash-free). The pyrolysis yields measured in this work are believed to be similar to those that would occur in an industrial entrained-flow gasifier since biomass pyrolysis yields depend heavily on heating rate and temperature. A refractory biomass tar yield near 1-2 wt% (dry, ash-free) was measured. Limited pyrolysis experiments were performed with corn stover since it consistently clogged the feed tube by pyrolyzing early in the feed tube near the burner. Biomass pyrolysis was modeled using the Chemical Percolation Devolatilization (CPD) model assuming that biomass pyrolysis occurs as a weighted average of its individual components (cellulose, hemicellulose, and lignin). Thermal cracking of tar into light gas was included using a kinetic model from the literature. Although the model correctly predicted that the measured biomass pyrolysis yields would be comprised almost entirely of gas, the model over-predicted the char yields at complete pyrolysis (≥ 60ms) by 6.2 to 8.6 wt% daf. These results are still encouraging considering the general nature of the pyrolysis model. The apparent CO_2 char gasification rates were measured for Poplar sawdust (~100 μm) in a pressurized flat-flame burner reactor at total pressures of 10 to 15 atm. The gas temperature and bulk CO_2 partial pressure ranges in these gasification experiments were 1186-1891 K and 4.3-13.5 atm, respectively. Particle residence time varied from 67 to 308 ms. Due to the highly volatile nature of biomass, pyrolyzed Poplar sawdust char was re-injected during gasification experiments to measure statistically meaningful extents of reaction. The CO_2 gasification rates for the two biomass chars were fit to a global 1st-order model.

1. Introduction.

Biomass as an energy source will likely play an increasing role in the future since political pressure has been growing recently to provide cleaner energy amid growing concerns about air quality and global climate change. For example, the European Union announced its intention to have 20% of its overall energy deriving from renewable sources by 2020 (Matsumoto et al., 2009). One way that biomass can be transformed into useful products such as energy and chemicals is through gasification, which converts any hydrocarbon to a mixture of hydrogen and carbon monoxide, the desired products, and CO_2 and H_2O through partial oxidation.

Many complex processes are involved in the gasification of a carbonaceous fuel such as drying, pyrolysis, and char gasification. The pyrolysis of biomass will be studied in this research since knowledge of volatile and char yields is necessary to provide the initial condition for gasification of the char residue (Flagan and Seinfeld, 1988), which is slow and therefore rate-controlling. The gasification rates of Poplar sawdust char are also measured in this research since a better understanding of the gasification reactivity of this fuel will enable the prediction of residence time and temperature requirements for complete reaction in conditions similar to those in entrained flow gasifiers. Although fluidized-bed technology is currently the most common for the thermal conversion of biomass, the data presented in this paper can aid in any planned entrained flow gasifiers. In addition, the presented data will provide a test case to evaluate both existing and future models at a wide range of temperatures at high heating-rate conditions.

2. Experimental Procedure

Samples. The biomass samples studied in this research were barkless Poplar sawdust, straw, switchgrass, and pelletized corn stover. The chosen feed stocks include energy crops as well as both woody and agricultural residues. The ultimate and proximate analyses of the biomass samples were performed at Brigham Young University and a summary of the results is included in Table 1. A Leco TruSpec Micro instrument was utilized in the ultimate analyses of the biomass samples. Sulfur was below the detection levels of the instrument for all biomass feed stocks, excluding corn stover.

The 4 biomass samples were ground using an electric wheat grinder (Blendtec Kitchen Mill) and sieved to collect the 45-75 μm size range. These small biomass particles were used in pyrolysis experiments in order to assume no interparticle temperature gradients for modeling purposes and to ensure a high initial heating rate of the particles.

Table 1. Ultimate and proximate analyses of the biomass feed stocks

Sample	Moisture[a] (wt%)	Ash (wt%, dry)	Volatiles (wt%, daf[b])	C (wt%, daf)	H (wt%, daf)	N (wt%, daf)	O[c] (wt%, daf)	S (wt%, daf)
Poplar Sawdust	2.38	0.82	88.85	48.84	5.91	0.11	45.14	-[d]
Straw	4.39	4.93	85.66	47.56	5.94	0.44	46.05	-[d]
Switchgrass	5.62	8.23	86.18	46.40	5.93	0.53	47.14	-[d]
Corn Stover	3.15	23.46	81.43	46.46	5.85	1.35	46.32	0.01

[a]as received basis. [b]daf = dry and ash-free basis. [c]calculated by difference. [d]below detection limits

Apparatus and Operation. A flat-flame burner (FFB) reactor operating at atmospheric pressure was used to study the pyrolysis of Poplar sawdust, straw, switchgrass, and corn stover in a fuel-rich flame using particle residence times less than 1 second. A pressurized flat-flame burner (HPFFB) reactor was used in the CO_2 gasification experiments for Poplar char. Its operation is very similar to that of the FFB reactor, except it operated at a total pressure up to 15 atm. Schematics of the FFB and HPFFB reactors appear in Figure 1. Flat-flame burners are useful since they provide particle heating rates around 10^5 K/s, which approaches the particle heating rates of about 10^6 K/s which are common in commercial, entrained-flow combustors and gasifiers (Fletcher et al., 1997).

The flat-flame burners use hundreds of small-diameter tubes to create many diffusion flamelets by feeding gaseous fuel through the tubes while introducing oxidizer in-between the tubes.

The numerous small flamelets create a flat flame a few millimeters above the burner. Particles were entrained in nitrogen and carried to the middle of the burner surface through a small metal tube (~0.050" ID). The particles then underwent thermal conversion while traveling upward in laminar flow for a known residence time before the particles were quickly quenched with nitrogen in a water-cooled collection probe. A virtual impactor and cyclone in the collection system separated the char aerodynamically while the soot/tar was collected on glass filters. Permanent gases passed through the filters and were released in a ventilation hood.

Particle residence times in the flat-flame burner reactors were calculated using particle velocities measured by a high-speed camera (Kodak EktaPro) and controlled by adjusting the height of the collection probe above the burner. Low particle feeding rates near 0.5 g/hr were used to ensure single-particle behavior, and to prevent clogging. The gaseous fuel supplied to both the FFB and HPPFB was mainly CO with a trace amount of H_2 to stabilize the flame. Additional details of the reactors have been reported elsewhere (Ma, 1996; Lewis, 2011; Shurtz, 2011).

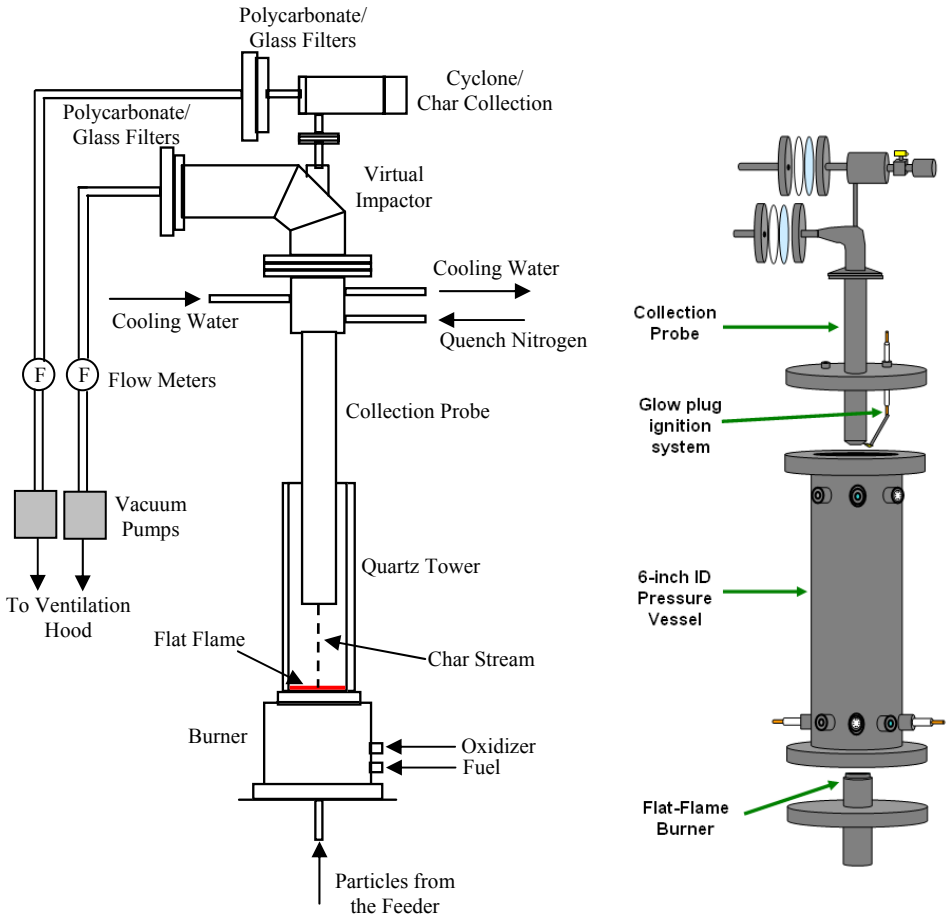

Figure 1. Schematics of FFB (left) and HPFFB reactors (right) (Shurtz, 2011).

The non-isothermal centerline gas temperature profiles in both the FFB and the HPFFB were obtained through temperature measurements corrected for radiation losses from a B-type thermocouple bead using equations that have been documented previously (Lewis, 2011). The different gas conditions in this paper are identified by the maximum gas temperature measured in

each profile. Biomass pyrolysis experiments were conducted at the 1163 K condition in the FFB, and the measured centerline gas temperature profile of this condition is shown in Figure 2.

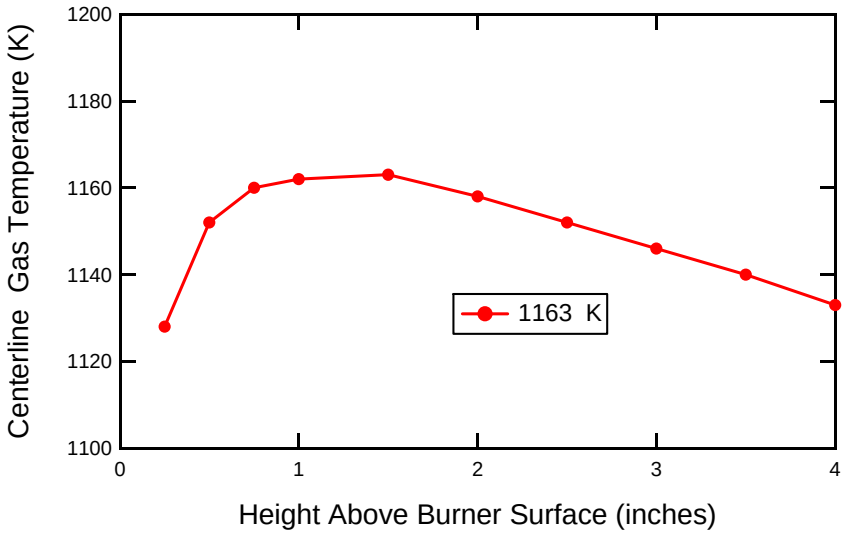

Figure 2. Centerline gas temperature profile of biomass pyrolysis experiments in FFB.

The fuel-rich CO_2 gasification experiments in the HPFFB were conducted at gas conditions where the post-flame environment was composed of ~40 and 90 mol% CO_2. Additional details of the gas conditions, as well as centerline temperature profiles, are included elsewhere (Lewis, in progress 2013). The gasification post-flame environments in this study contained CO_2 with ~10 mol% CO, which is known to be an inhibitor to the CO_2/char gasification reaction. The measured CO_2 gasification rates of Poplar sawdust char in this study are still valuable since commercial gasification typically occurs in an environment containing both CO_2 and CO. In addition, it has been shown that the retarding influence of CO on the CO_2/char gasification reaction has the most pronounced effect at conditions of lower temperature and higher CO/CO_2 atomic ratios than studied here (Turkdogan and Vinters, 1970).

3. Results and Discussion

Biomass Pyrolysis Mass Release. Ground and sized (45-75 μm) raw samples of Poplar sawdust, straw, switchgrass, and corn stover were fed separately through the FFB reactor at atmospheric pressure in order to measure pyrolysis yields of char, tar, and light gas at different residence times at a gas condition with a peak temperature of 1163 K. Figure 3 shows biomass particles being pyrolyzed in the FFB during these experiments.

Figure 4 shows a summary of the measured mass release during the FFB pyrolysis experiments at atmospheric pressure using a peak gas temperature of 1163 K. The mass release in Figure 4 represents the percentage of the particle's mass on a dry ash-free (daf) basis that volatilized during pyrolysis. Mass release was calculated using a mass balance, using weights of both raw biomass fed and char that was collected after the run. The Poplar sawdust had the highest mass release (~ 99 wt% daf) while straw had the lowest (~93 wt%).

Figure 3. Biomass particles being pyrolyzed in the FFB reactor.

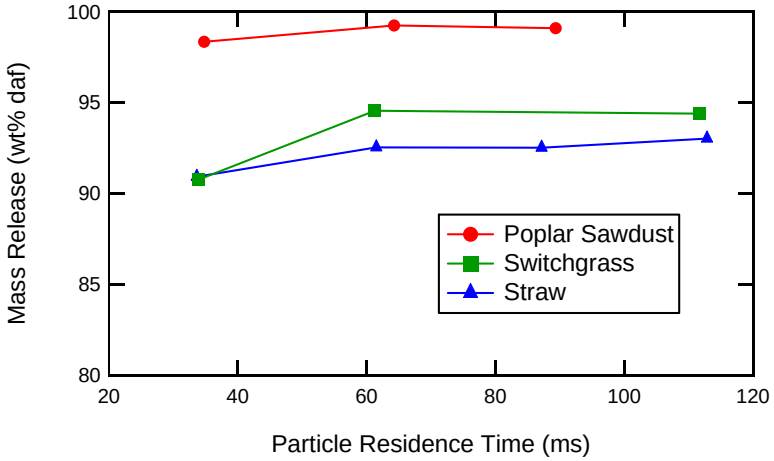

Figure 4. Mass release (daf) of the biomass pyrolysis experiments at atmospheric pressure at a peak gas temperature of 1163 K in the FFB reactor.

The data points at the earliest residence time (~ 35 ms) in Figure 4 were the only experiments where partial pyrolysis of the biomass fuels was measured. Obtaining additional data at partial pyrolysis was beyond the ability of the atmospheric flat-flame burner since this would require lower temperatures and/or shorter particle residence times. Trying to change gas flow rates to the burner to decrease gas temperatures below 1163 K resulted in an unstable flame, and obtaining shorter residence times than 35 ms would require a distance less than 1" between burner and collection probe (making the temperature history difficult to classify). Poplar sawdust, switchgrass, and straw all reached full pyrolysis at particle residence times greater than ~60 ms, which is indicated in Figure 4 by the asymptotic mass release values.

Corn stover experiments were not summarized in Figure 4 because only limited experiments could be run. This biomass fuel posed serious feeding problems since it pyrolyzed in the feed tube near the burner and consistently clogged the feed tube. Using about 1.5 times the usual carrier N_2 in the feed tube allowed corn stover to be fed without clogging, which allowed one data point of full

pyrolysis of corn stover at a high heating-rate condition. The pyrolysis mass release of corn stover at high heating-rate conditions was 93.05 wt% (daf basis).

It was difficult to measure partial pyrolysis conditions for the biomass feed stocks in the FFB reactor, but the same biomass feed stocks (Poplar sawdust, switchgrass, & corn stover) were fed in a drop tube reactor at lower temperatures and have been documented elsewhere (Maghzi and Rizeq, 2011). It is important to note that the ash percentages in Table 1 are only valid for the runs done in the FFB reactor. Slightly larger biomass particles that had different ash fractions were fed in the drop tube experiments.

Figure 5 shows the difference in biomass mass release at low and high heating rate conditions for Poplar sawdust, straw, switchgrass, and corn stover. The low heating-rate mass release values in Figure 5 came from an ASTM volatiles test (see Table 1). The high heating-rate mass release values came from atmospheric FFB experiments where complete pyrolysis was obtained. The difference between low and high heating rate mass release values was greatest for corn stover (11.6 wt% daf difference), followed by Poplar sawdust (10.3 wt% daf difference), switchgrass (8.3 wt% daf difference), and straw (7.0 wt% daf difference). Other researchers have also noticed a difference in volatile content of biomass when comparing data from low and high heating-rate conditions. For example, Borrego et al. (2009) measured up to 12% greater volatile yields than the ASTM volatiles test when pyrolyzing wood chips, forest residues, and rice husks at high heating rate in a drop tube furnace.

Measuring pyrolysis yields in the flat-flame burner under high particle heating-rate conditions is believed to be an accurate representation of the pyrolysis that occurs for small particles in entrained-flow combustors and gasifiers where initial particle heating rates of 10^6 K/s are common (Fletcher et al., 1997).

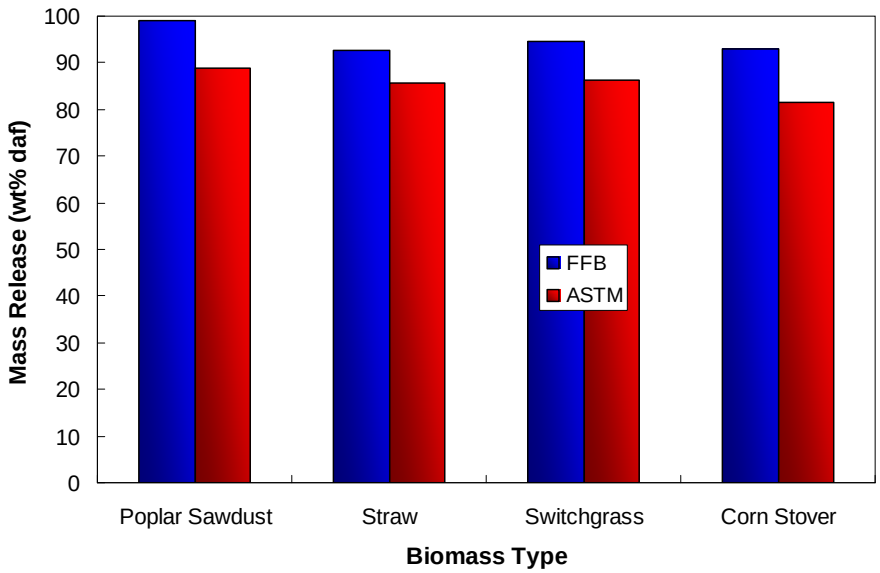

Figure 5. Comparison of mass release (daf basis) at low and high heating-rate conditions for Poplar sawdust, straw, switchgrass, and corn stover.

Tar and Gas Yields of Biomass Pyrolysis. Tar and gas yields from the biomass atmospheric FFB experiments appear in Figure 6. The peak gas temperature in these experiments was 1163 K. The tar yields were calculated based on the mass that collected on the water-cooled glass filters in the FFB collection system (see Figure 1). Note that the gas yields in Figure 6b were determined by

difference, i.e., (100% – char yield (daf)% – tar yield (daf)%). The tar and gas yields in Figure 6 were calculated on a basis of dry ash-free biomass fed. The reported yields were based on a mass balance (i.e., tar yield = weight of collected tar/weight of daf biomass fed).

At a gas temperature of 1163 K in the FFB, very low tar yields were observed, especially considering that biomass tar yields can be as high as 75 wt% at certain conditions (Bridgwater, 2003). Thermal cracking of tar into light gas caused the low tar yields. Tar cracking becomes important above 800 K (Scott et al., 1988; Stiles and Kandiyoti, 1989) for biomass tars.

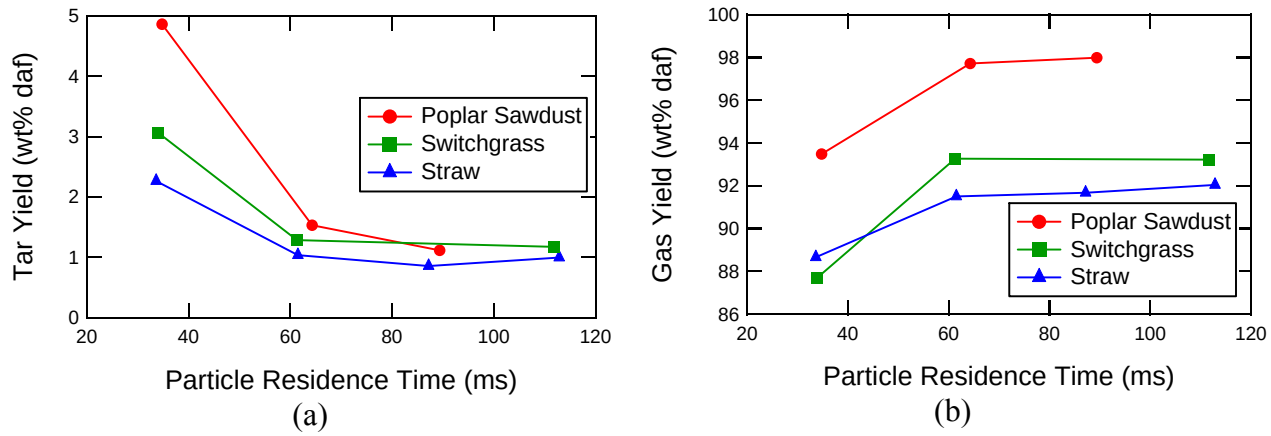

Figure 6. Yields (wt% daf) of (a) tar and (b) gas from biomass pyrolysis experiments in the atmospheric FFB at a peak gas temperature of 1163 K.

It is interesting to note that the tar yields from all the biomass pyrolysis experiments level off near 1 wt% (daf) in the FFB. It is suggested in the literature that there exists a small fraction of biomass tar that is or becomes refractory (Antal, 1983; Rath and Staudinger, 2001; Bridgwater, 2003; Di Blasi, 2008; Jarvis et al., 2011). Other researchers have shown that hotter reactor temperatures result in an increased fraction of aromatic compounds and condensed ring structures in the biomass tar (Stiles and Kandiyoti, 1989; Zhang et al., 2007; Jarvis et al., 2011). In order to test for refractory tar, Poplar sawdust was fed in the FFB at a condition where the peak gas temperature was near 1750 K using a particle residence time near 75 ms. A decreased tar yield was not measured at the 1750 K condition, suggesting that the asymptotic biomass tar yields in Figure 6a were the result of collecting refractory tar.

Tar and gas yields of corn stover were not included in Figure 6 since limited experiments were conducted using corn stover due to feeding problems, as mentioned previously. The asymptotic tar and gas yields from the corn stover experiments were 2.2 wt% and 90.9 wt% (daf), respectively.

Biomass Pyrolysis Modeling. The basis of the biomass CPD model is to combine the predicted pyrolysis yields of cellulose, hemicellulose, and lignin as a weighted average in order to predict the pyrolysis yields of a biomass species. The biomass content of the studied biomass fuels was therefore measured (UC Davis Analytical Lab) and the results are summarized in Table 2.

The biomass CPD model (Lewis and Fletcher, 2013) has been shown to accurately model the pyrolysis yields (i.e., char, tar, & gas) of sawdust when used in combination with a tar-cracking model above 500 °C. In this work, the performance of the biomass CPD model was evaluated for Poplar sawdust, as well as straw and switchgrass when using the tar cracking model of Fagbemi et

al. (2001). The values of A and E that were used in Fagbemi's model were 4.28 x 10^6 s^{-1} and 107.5 kJ/mol, respectively.

Table 2. Meausured biomass fractions of Poplar sawdust, straw, and switchgrass

Biomass Component	Poplar Sawdust	Straw	Switchgrass
Cellulose (wt%)	62.99	46.25	46.25
Hemicellulose (wt%)	24.21	41.48	41.48
Lignin (wt%)	12.90	12.28	12.28

The comparison between measured and modeled biomass pyrolysis yields of Poplar sawdust and straw are summarized in Figures 7a and b, respectively. The biomass CPD model when used in combination with the tar cracking model of Fagbemi et al. (2001) essentially predicted full pyrolysis after the first measured collection point, just as was measured during experimentation in the FFB at 1163 K. Although the model correctly predicted that the measured biomass yields would be comprised almost entirely of gas, the model over-predicted the char yield at complete pyrolysis (≥ 60ms) by 8.6 and 6.2 wt% daf for Poplar sawdust and straw, respectively. However, these results are still encouraging considering the general nature of the model.

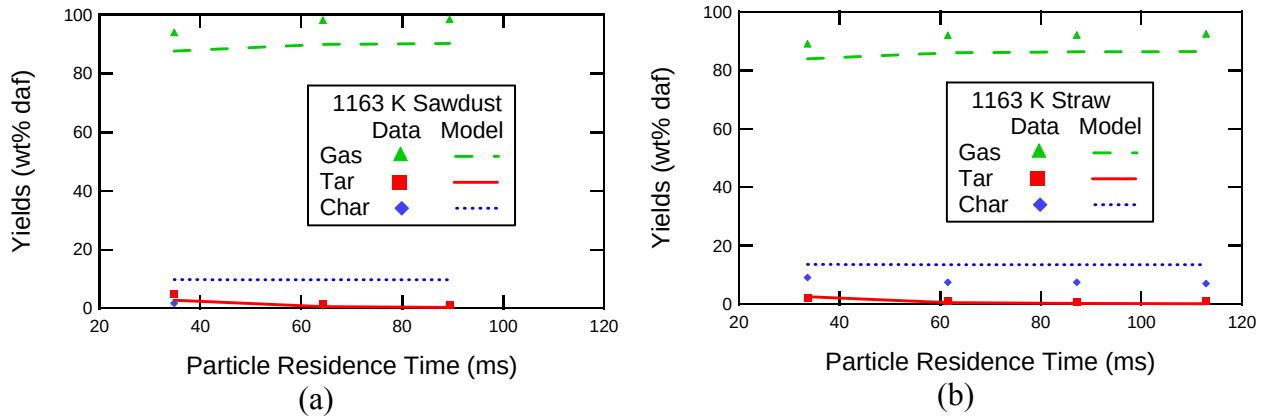

Figure 7. Comparison of measured and modeled (a) Poplar sawdust and (b) straw pyrolysis yields in the FFB at 1 atm and peak gas temperature of 1163 K.

The comparison between measured and modeled biomass pyrolysis yields of switchgrass is summarized in Figure 8a when using the CPD model in combination with Fagbemi's tar cracking model. Similarly as with Poplar sawdust and straw, the model over-predicted the fully-pyrolyzed char yields (6.8 wt% daf), but predicted essentially complete pyrolysis at residence times ≥ 60 ms, as was measured in the FFB reactor. Figure 8b is a comparison of measured and modeled pyrolysis yields of switchgrass solely from the CPD model (without use of a Fagbemi's tar cracking model). This comparison demonstrates the importance of combining the results of the CPD model with a tar cracking model, since tar cracking reactions greatly affect tar and gas yields above 500 °C.

The ability of the CPD model (when used in combination with a tar cracking model) to correctly predict the pyrolysis yields from a range of biomass feed stocks is encouraging. It is also interesting to note that although the tar cracking kinetic parameters used in Fagbemi's model were based from sawdust data (Liden et al., 1988), they accurately predicted the tar cracking of other biomass fuels like straw and switchgrass.

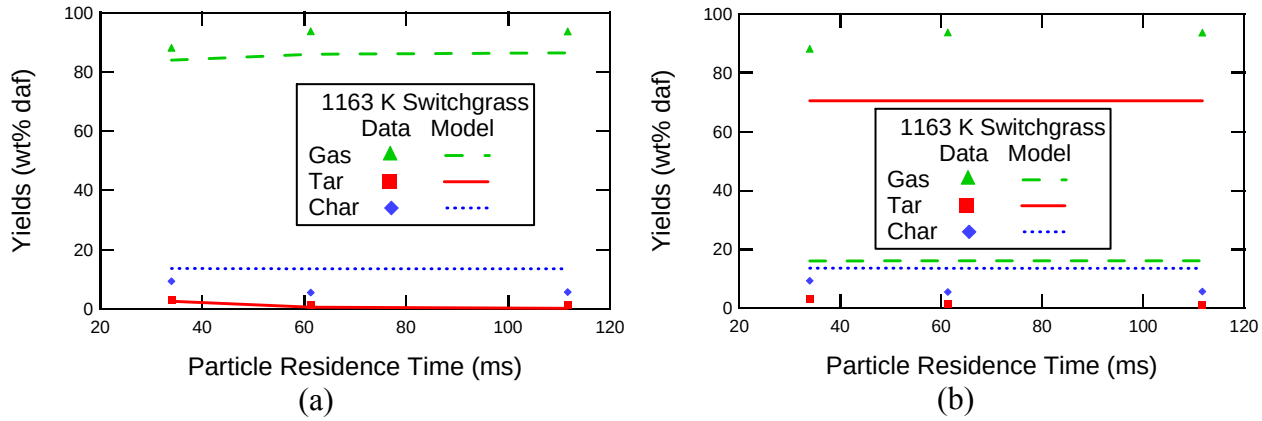

Figure 8. Comparison of measured and modeled switchgrass pyrolysis yields in the FFB at 1 atm and peak gas temperature of 1163 K (a) with and (b) without use of Fagbemi's tar cracking model.

CO_2 Gasification Rates of Poplar Sawdust Char. The apparent CO_2 gasification rates of Poplar sawdust char were measured in the HPFFB at conditions near 40 and 90 mol% CO_2 at total pressures of 10 and 15 atm. The gas temperature and bulk CO_2 partial pressure ranges in these gasification experiments were 1186-1891 K and 4.3-13.5 atm, respectively. Particle residence time varied from 67 to 308 ms. The HPFFB sawdust gasification experiments involved re-injecting pyrolyzed sawdust char that was generated at high heating-rate conditions at 1 atm in the Bench Scale Gasifier (BSG) drop tube reactor (Maghzi and Rizeq, 2011). The method of re-injecting fully-pyrolyzed chars to measure char oxidation data has been used previously by others (Hurt et al., 1998; Shurtz, 2011). Considering the highly volatile nature of biomass solely from pyrolysis, the re-injection approach was used since measuring statistically different extents of gasification in the HPFFB would have been difficult to impossible otherwise. A second reason the Poplar sawdust char was generated in the BSG and not in BYU's HPFFB was due to resource constraints. The BSG quickly produced biomass char due to its ability to feed biomass at 30 g/hr, which is substantially faster than the ~0.7 g/hr maximum feed rate of the HPFFB. The Poplar sawdust char that acted as a feed stock for HPFFB CO_2 gasification experiments had a mass mean of 100.7 μm, and is shown in Figure 9. These SEM images were taken at BYU using a FEI XL30 ESEM with a FEG emitter.

The Poplar sawdust char was generated by feeding raw Poplar sawdust in the BSG reactor at a gas temperature near 980 K for ~740 ms. The char was naturally spherical due to the high heating-rate pyrolysis conditions of the BSG reactor. Other researchers (Zhang et al., 2006; Dupont et al., 2008) have also noticed that spherical sawdust char resulted when pyrolyzing sawdust at conditions of high heating rate. Spherical sawdust char is only characteristic of sawdust pyrolyzed at high heating rates since Cetin et al. (2004) did not observe any major morphological changes of sawdust pyrolyzed at a low heating rate of 20 K/s.

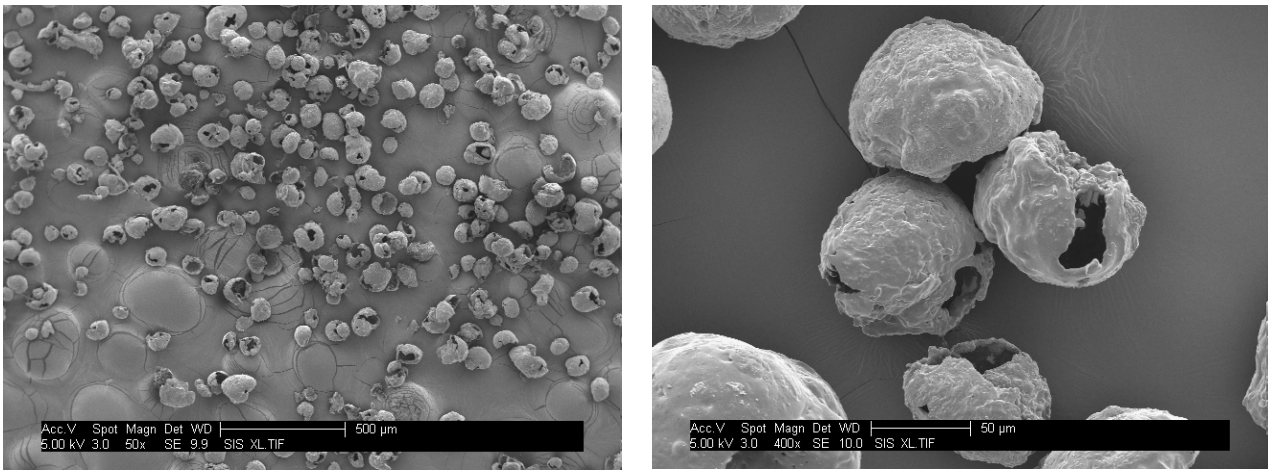

(a) (b)

Figure 9. SEM images of pyrolyzed Poplar sawdust char used in HPFFB CO_2 gasification experiments.

Gasification Model. Although more complicated models exist (Liu and Niksa, 2004; Shurtz, 2011), the char mass release data from the CO_2 gasification experiments in the HPFFB reactor were modeled with a simple first-order global model where the rate is normalized by particle external surface area:

$$\frac{dm_p}{dt}\cdot\frac{1}{A_p} = k_{rxn}\cdot P_{CO2,surf} = \left[A\cdot\exp\left(\frac{-E}{R\cdot T_p}\right)\right]\cdot P_{CO2,surf} \quad (1)$$

where m_p is the particle mass, t is time, A_p is the external surface area of the assumed-spherical particle, k_{rxn} is the rate constant of CO_2 gasification, $P_{CO2,\,surf}$ is the partial pressure of CO_2 at the particle surface, A is the pre-exponential factor, E is activation energy, R is the ideal gas constant, and T_p is the particle temperature. The particle diameter used to calculate A_p for the Poplar char was 100.7 µm. The rate in Equation (1) was integrated using the Explicit Euler method for integration in an Excel spreadsheet, and is negative since the particles lost mass during CO_2 gasification. The kinetic parameter A was determined by minimizing the sum-squared error between predicted and measured gasification mass release data using the Excel Solver. The activation energy was varied using a trial-and-error approach in order to minimize the sum-squared error between predicted and measured data.

Since only the gas temperature (T_{gas}) was measured, T_p was solved for each time step using an energy balance of the particle:

$$m_p\cdot C_p\cdot\frac{dT_p}{dt} = h_c\cdot A_p\cdot(T_{gas}-T_p)+\varepsilon_p\cdot\sigma\cdot A_p\cdot({T_{surr}}^4-{T_p}^4)+\frac{dm_p}{dt}\cdot\Delta H_{rxn} \quad (2)$$

where C_p is the heat capacity of the particle, h_c is the heat transfer coefficient ($Nu\cdot k_{gas}/d_p$), ε_p is the emissivity of the char particle (ε_p =0.8 with the assumption that it was similar to that of coal char) (Fletcher, 1989), σ is the Stefan–Boltzmann constant (5.67 x 10^{-12} W/cm^2/K), T_{surr} is the temperature of the surroundings (500 K), and ΔH_{rxn} is the heat of reaction for the CO_2 gasification reaction. The left-hand side of Equation 2 was set equal to zero since steady state was assumed during the small time steps of ~ 0.15 ms. The first term on the right-hand side of Equation 2 represents the particle

heating up from convective heat transfer. The second term in Equation 2 is the radiative heat transfer from the particle, which is negative when $T_p > T_{surr}$. The last term in Equation 2 takes into account the heat from the reacting particle which is negative (from the dm_p/dt term) due to the endothermic CO_2 gasification reaction.

Although the model does not take pore diffusion into account, it does consider film diffusion, which allowed $P_{CO2,surf}$ to be solved for explicitly:

$$P_{CO2,surf} = \frac{\nu \cdot h_m \cdot P_{CO2,\infty}}{R \cdot T_{gas}\left[k_{rxn} + \frac{\nu \cdot h_m}{R \cdot T_p}\right]} \quad (3)$$

where v is the mass of carbon (in grams) that react per mole of reactant, h_m is the mass transfer coefficient ($Sh \cdot D_{AB}/d_p$), and $P_{CO2,\infty}$ is the partial pressure of CO_2 in the bulk gas. In the case of CO_2 gasification, v was (12 g C/ mol CO_2) from the following reaction:

$$C + CO_2 \rightarrow 2\ CO$$

Additional details of the first-order model are reported elsewhere (Lewis, 2011). In this work, values for k_{gas} and D_{AB} were changed to account for the different gas conditions when modeling the 90 mol% CO_2 gas conditions of the HPFFB reactor.

Modeling Results. The kinetic parameter A was regressed for Poplar sawdust char using different combinations of measured mass release CO_2 gasification data from the HPFFB reactor. For ease of explanation, Cases #1 through #3 will be used to identify which Poplar mass release data were used to regress A. As summarized in Table 3, Cases #1 and #2 included the mass release data at conditions where the post-flame environment in the HPFFB was near 40 and 90 mol%, respectively. Case #3 included all the Poplar char mass release data from Cases #1 and #2.

Table 3. Identifier of which mass release data from the HPFFB was used to optimize A & E

	Total Pressure (atm); Peak T_{gas} (K)	**mol% CO_2 in post-flame environment**
Case #1	15 atm; 1734 K 15 atm; 1968 K	~40
Case #2	15 atm; 1723 K 15 atm; 1848 K	~90
Case #3	all data from Cases #1 & #2	all data from Cases #1 & #2

The optimized A and E values for the three data sets are summarized in Table 4. The parity plots shown in Figure 10 show how the measured Poplar mass release data (on a char basis) compared with that predicted by the 1st-order gasification model using kinetic parameters in Table 4. Also included in Table 4 is the range of $P_{CO2,surf}$ and T_p values of the experimental data from which A and E values were optimized, as calculated by Equations 2 and 3.

The fits of the 1st-order gasification model in Figure 10 are reasonable considering the simplicity of the model. The discrepancy between modeled and measured mass release values for the Poplar sawdust char would likely be lessened by adding complexities to the model (Equation 1). For example, adding an effectiveness factor to the model would allow insight into the effect of pore diffusion on the measured rates. Currently, the reaction order, n, of $P_{CO2,surf}$ is unity in Equation 1, but allowing n to vary would likely improve the fit of the model. Also, rates were normalized by

external surface area. Perhaps normalizing the rates by internal surface area would improve the fits of the model, although this would become complicated since surface area does not likely stay constant during conversion.

Table 4. 1st-order kinetic rate coefficients for CO_2 gasification of Poplar sawdust char

Poplar data used to optimize *A* & *E*	***A*** $\left[\frac{g\ Carbon}{cm^2 \cdot s \cdot atm\ CO_2}\right]$	***E*** **(kJ/mol)**	$P_{CO2,surf}$ **(atm)**	T_p **(K)**
Case #1	378.365	162.5	4.2 - 6.0	1199 - 1514
Case #2	0.193	80	9.9 – 12.4	1084 – 1450
Case #3	3.548	110	4.2 - 12.4	1084 - 1514

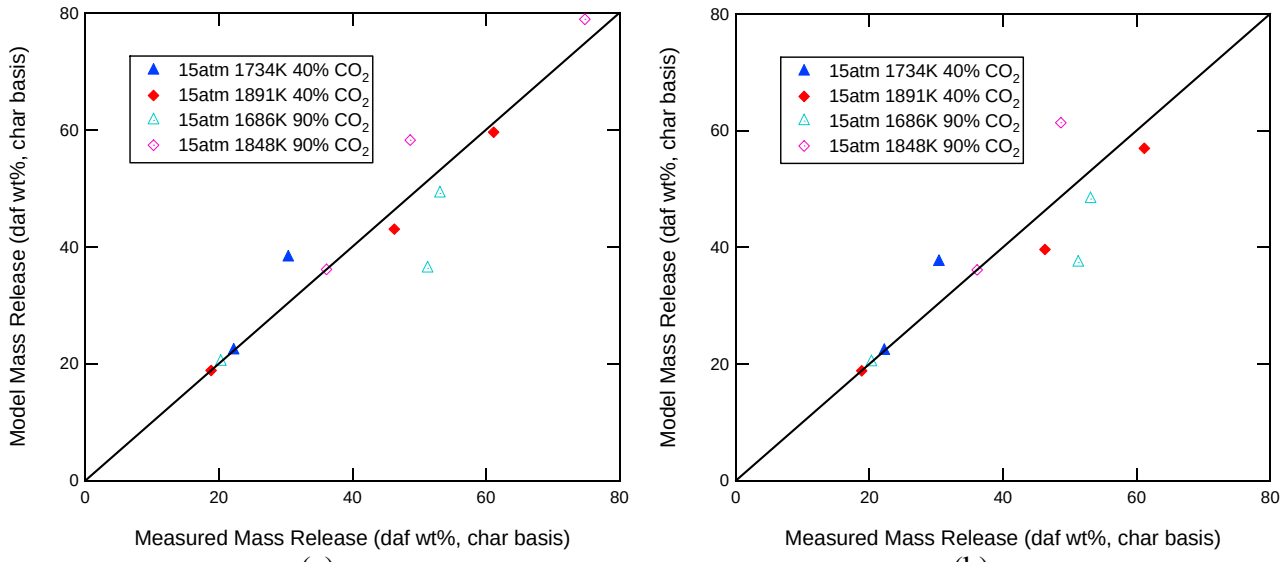

Figure 10. Parity plot of HPFFB gasification Poplar sawdust char data with 1st-order model. Figure (a) shows the fit when *A* and *E* were solved separately for the 40 mol% and 90 mol% CO_2 conditions (Cases #1 & #2) while Figure (b) is the fit when *A* and *E* were solved including data from all 4 gas conditions (Case #3).

Reaction Regime of Measured Data. It is important when measuring kinetics at high temperature to make sure that the measurements are not entirely controlled by film diffusion. The chi factor (Smith et al., 1994), χ, was calculated for all the conditions since it provides an indication of the effect of film diffusion. It is defined as the measured rate divided by the maximum rate under film-diffusion control and can be calculated by the following equation:

$$\chi = \left(\frac{k_{rxn} \cdot P_{CO2,surf}}{\nu \cdot h_m \cdot \left(C_{CO2,\infty}\right)} \right) = \frac{k_{rxn} \cdot P_{CO2,surf}}{\nu \cdot h_m \cdot \left(\frac{P_{CO2,\infty}}{R \cdot T_{gas}} \right)} \tag{4}$$

where $C_{CO2,\infty}$ is defined as the concentration of CO_2 in the bulk phase. The surface reaction controls when χ is much less than 1. Film diffusion controls entirely when χ approaches 1. In the HPFFB CO_2 gasification experiments feeding Poplar sawdust char, that maximum χ value was 0.164. These χ values mean that the measured kinetics took place under Zone II conditions (Smith et al., 1994), which is a transition region between surface-reaction control and film-diffusion control. The gasification kinetics of Poplar sawdust char measured in the HPFFB were likely similar to those in a commercial entrained-flow gasifier since these commercial reactors operate in Zone II conditions as well. Additional evidence that the Poplar sawdust char reacted under Zone II conditions was that both their particle diameter and density varied.

4. Conclusions

The pyrolysis of four biomass feed stocks (Poplar sawdust, straw, switchgrass, and corn stover) was studied at conditions of high initial particle heating rates at atmospheric pressure in a flat-flame burner reactor. Pyrolysis yields of tar, char, and light gas were reported for each of the biomass feed stocks although only limited experiments could be conducted with corn stover since it consistently clogged the feed line by pyrolyzing inside the feed tube near the burner. A refractory biomass tar yield near 1-2 wt% (dry, ash-free) was measured. The mass release of the biomass samples at high heating-rate conditions in the flat-flame reactor exceeded their respective ASTM volatiles value by 7.0 to 11.6 wt% (dry, ash-free). The pyrolysis yields measured in this work are believed to be similar to those that would occur in an industrial entrained-flow gasifier or combustor.

Biomass pyrolysis was modeled using the Chemical Percolation Devolatilization (CPD) model assuming that biomass pyrolysis occurs as a weighted average of its individual components (cellulose, hemicellulose, and lignin). The CPD model was combined with a tar-cracking model from the literature since the pyrolysis yields in the flat-flame burner reactor were measured at temperatures exceeding 500 °C. The predictions of the model are encouraging since the model well approximated the pyrolysis yields of straw and switchgrass, in addition to sawdust which has been compared previously.

The apparent CO_2 gasification rates were measured for Poplar sawdust char in a pressurized flat-flame burner reactor at total pressures of 10 to 15 atm in conditions near 40 and 90 mol% CO_2. Due to the highly volatile nature of biomass, pyrolyzed Poplar sawdust char was re-injected during gasification experiments to measure statistically meaningful extents of reaction. The CO_2 gasification rates for the two biomass chars were fit to a global 1st-order model, and kinetic parameters were presented.

Acknowledgements

This research was funded in part by Grant 2009-10006-06020 from the US Department of Agriculture/NIFA. However, any opinions, findings, conclusions or other recommendations expressed herein are those of the authors and do not necessarily reflect the views of NIFA. The authors wish to acknowledge BYU's Microscopy lab for their assistance in obtaining the SEM images.

References

Antal, M. J., "Effects of Reactor Severity on the Gas-Phase Pyrolysis of Celulose-Derived and Kraft Lignin-Derived Volatile Matter," *Industrial & Engineering Chemistry Product Research and Development,* **22**(2), 366-375 (1983).

Borrego, A. G., L. Garavaglia and W. D. Kalkreuth, "Characteristics of High Heating Rate Biomass Chars Prepared under N_2 and CO_2 Atmospheres," *International Journal of Coal Geology,* **77**(3-4), 409-415 (2009).

Bridgwater, A. V., "Renewable Fuels and Chemicals by Thermal Processing of Biomass," *Chemical Engineering Journal,* **91**(2-3), 87-102 (2003).

Cetin, E., B. Moghtaderi, R. Gupta and T. F. Wall, "Influence of Pyrolysis Conditions on the Structure and Gasification Reactivity of Biomass Chars," *Fuel,* **83**(16), 2139-2150 (2004).

Di Blasi, C., "Modeling Chemical and Physical Processes of Wood and Biomass Pyrolysis," *Progress in Energy and Combustion Science,* **34**(1), 47-90 (2008).

Dupont, C., J. M. Commandre, P. Gauthier, G. Boissonnet, S. Salvador and D. Schweich, "Biomass Pyrolysis Experiments in an Analytical Entrained Flow Reactor between 1073 K and 1273 K," *Fuel,* **87**(7), 1155-1164 (2008).

Fagbemi, L., L. Khezami and R. Capart, "Pyrolysis Products from Different Biomasses: Application to the Thermal Cracking of Tar," *Applied Energy,* **69**(4), 293-306 (2001).

Flagan, R. C. and J. H. Seinfeld, Fundamentals of Air Pollution Engineering, Englewood Cliffs, New Jersey, Prentice-Hall, Inc., pp. 59-166 (1988).

Fletcher, T. H., "Time-Resolved Temperature-Measurements of Individual Coal Particles During Devolatilization," *Combustion Science and Technology,* **63**(1-3), 89-105 (1989).

Fletcher, T. H., J. L. Ma, J. R. Rigby, A. L. Brown and B. W. Webb, "Soot in Coal Combustion Systems," *Progress in Energy and Combustion Science,* **23**(3), 283-301 (1997).

Hurt, R., J. K. Sun and M. Lunden, "A Kinetic Model of Carbon Burnout in Pulverized Coal Combustion," *Combustion and Flame,* **113**(1-2), 181-197 (1998).

Jarvis, M. W., T. J. Haas, B. S. Donohoe, J. W. Daily, K. R. Gaston, W. J. Frederick and M. R. Nimlos, "Elucidation of Biomass Pyrolysis Products Using a Laminar Entrained Flow Reactor and Char Particle Imaging," *Energy & Fuels,* **25**, 324-336 (2011).

Lewis, A., "Gasification of Biomass and Petroleum Coke by CO_2 at High Heating Rates and Elevated Pressure," PhD Dissertation, Brigham Young University (in progress 2013).

Lewis, A. D., "Sawdust Pyrolysis and Petroleum Coke CO_2 Gasification at High Heating Rates," Master's Thesis, Brigham Young University (2011).

Lewis, A. D. and T. H. Fletcher, "Prediction of Sawdust Pyrolysis Yields from a Flat-Flame Burner Using the CPD Model," *Energy & Fuels,* **27**, 942-953 (2013).

Liden, A. G., F. Berruti and D. S. Scott, "A Kinetic-Model for the Production of Liquids from the Flash Pyrolysis of Biomass," *Chemical Engineering Communications,* **65**, 207-221 (1988).

Liu, G. S. and S. Niksa, "Coal Conversion Submodels for Design Applications at Elevated Pressures. Part II. Char Gasification," *Progress in Energy and Combustion Science,* **30**(6), 679-717 (2004).

Ma, J., "Soot Formation During Coal Pyrolysis," PhD Dissertation, Brigham Young University (1996).

Maghzi, S. and G. Rizeq, "Experimental Study of Biomass Pyrolysis in an Entrained Flow Reactor," Western States Section of the Combustion Institute, Riverside, CA (2011).

Matsumoto, K., K. Takeno, T. Ichinose, T. Ogi and M. Nakanishi, "Gasification Reaction Kinetics on Biomass Char Obtained as a by-Product of Gasification in an Entrained-Flow Gasifier with Steam and Oxygen at 900-1000 Degrees C," *Fuel,* **88**(3), 519-527 (2009).

Rath, J. and G. Staudinger, "Cracking Reactions of Tar from Pyrolysis of Spruce Wood," *Fuel,* **80**(10), 1379-1389 (2001).

Scott, D. S., J. Piskorz, M. A. Bergougnou, R. Graham and R. P. Overend, "The Role of Temperature in the Fast Pyrolysis of Cellulose and Wood," *Industrial & Engineering Chemistry Research,* **27**(1), 8-15 (1988).

Shurtz, R., "Effects of Pressure on the Properties of Coal Char under Gasification Conditions at High Initial Heating Rates," PhD Dissertation, Brigham Young University (2011).

Smith, K. L., L. D. Smoot, T. H. Fletcher and R. J. Pugmire, The Structure and Reaction Processes of Coal, New York, Plenum Press (1994).

Stiles, H. N. and R. Kandiyoti, "Secondary Reactions of Flash Pyrolysis Tars Measured in a Fluidized-Bed Pyrolysis Reactor with Some Novel Design-Features," *Fuel,* **68**(3), 275-282 (1989).

Turkdogan, E. T. and J. V. Vinters, "Effect of Carbon Monoxide on the Rate of Oxidation of Charcoal, Graphite and Coke in Carbon Dioxide," *Carbon,* **8**, 39-53 (1970).

Zhang, J., H. Toghiani, D. Mohan, C. U. Pittman and R. K. Toghiani, "Product Analysis and Thermodynamic Simulations from the Pyrolysis of Several Biomass Feedstocks," *Energy & Fuels,* **21**(4), 2373-2385 (2007).

Zhang, Y., S. Kajitani, M. Ashizawa and K. Miura, "Peculiarities of Rapid Pyrolysis of Biomass Covering Medium- and High-Temperature Ranges," *Energy & Fuels,* **20**(6), 2705-2712 (2006).